The nutrient-sensing Rag-GTPase complex in B cells controls humoral immunity via TFEB/TFE3-dependent mitochondrial fitness

Xingxing Zhu[1], Yue Wu[2,3], Yanfeng Li[1], Xian Zhou[1], Jens O. Watzlawik[4], Yin Maggie Chen[5], Ariel L. Raybuck[6], Daniel D. Billadeau[5], Virginia Smith Shapiro[5], Wolfdieter Springer[4,7], Jie Sun[2,3], Mark R. Boothby[6], Hu Zeng[1,5,*]

[1]Division of Rheumatology, Department of Medicine, Mayo Clinic Rochester, MN 55905, USA

[2]Carter Immunology Center, University of Virginia, Charlottesville, VA 22908, USA

[3]Division of Infectious Diseases and International Health, Department of Medicine, University of Virginia, Charlottesville, VA 22908, USA

[4]Department of Neuroscience, Mayo Clinic, Jacksonville, FL 32224, USA

[5]Department of Immunology, Mayo Clinic Rochester, MN 55905, USA

[6]Department of Pathology, Microbiology & Immunology, Molecular Pathogenesis Division, Vanderbilt University Medical Center and School of Medicine, Nashville, TN 37232, USA

[7]Neuroscience PhD Program, Mayo Clinic Graduate School of Biomedical Sciences, Jacksonville, FL 32224, USA

*Corresponding author: Hu Zeng; E-mail: Zeng.hu1@mayo.edu

Supplementary Fig. 1

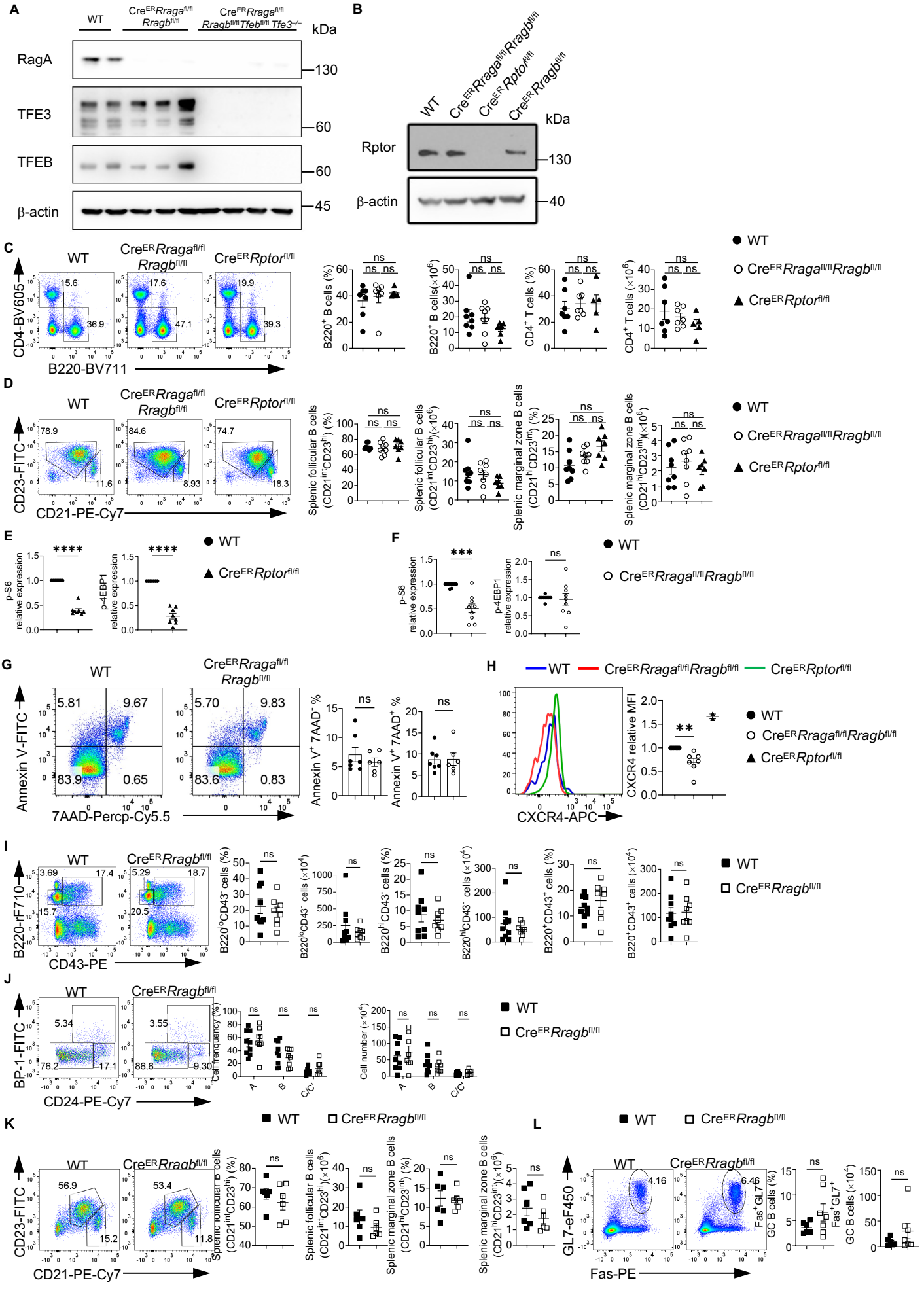

Supplementary Fig. 1. RagB deficiency doesn't affect early B cell development in BM and peripheral B cells. Expression of RagA, TFEB, TFE3 (A) and Raptor (B) was examined by immunoblot. (C) Representative flow plots of splenic $CD4^+$ T cells and $B220^+$ B cells from WT mice (n = 7), *Cre*^{ER}*Rraga*$^{fl/fl}$*Rragb*$^{fl/fl}$ (n = 7), and *Cre*^{ER}*Rptor*$^{fl/fl}$ (n = 5). (D) flow plots of splenic follicular B cells ($CD21^{int}CD23^{hi}$) or marginal zone ($CD21^{hi}CD23^{int}$) from WT mice (n = 8), *Cre*^{ER}*Rraga*$^{fl/fl}$*Rragb*$^{fl/fl}$ (n = 8), and *Cre*^{ER}*Rptor*$^{fl/fl}$ (n = 7). (E and F) Summaries of p-S6 and p-4EBP1 expressions in the B cells stimulated with LPS/IL-4/BAFF for 72 h and examined by immunoblot. E, WT mice (n = 7), and *Cre*^{ER}*Rptor*$^{fl/fl}$ (n = 8). F, WT mice (n = 9) and *Cre*^{ER}*Rraga*$^{fl/fl}$*Rragb*$^{fl/fl}$ (n = 9). (G) The percentages of Annexin V^+7-AAD^- and Annexin V^+7-AAD^+ B cells were examined by flow cytometry. WT mice (n = 7) and *Cre*^{ER}*Rraga*$^{fl/fl}$*Rragb*$^{fl/fl}$ (n = 6). (H) Expression of CXCR4 on BM $B220^{hi}CD43^-$ B cells. Right, the relative MFI of CXCR4 level on BM $B220^{hi}CD43^-$ B cells. WT mice (n = 7), *Cre*^{ER}*Rraga*$^{fl/fl}$*Rragb*$^{fl/fl}$ (n = 7), and *Cre*^{ER}*Rptor*$^{fl/fl}$ (n = 2). (I) Representative flow plots of bone marrow B220 and CD43 expression from WT (n = 9), and Cre^{ER}*Rragb*$^{fl/fl}$ (n = 8) mice. (J) Representative flow plots of BP-1 and CD24 expression in BM $B220^+CD43^+IgM^-$ B cell precursors from WT (n = 9) and Cre^{ER}*Rragb*$^{fl/fl}$ (n = 8) mice. (K) Representative flow plots of splenic follicular B cells ($CD21^{int}CD23^{hi}$) or marginal zone ($CD21^{hi}CD23^{int}$) from WT (n = 9) and Cre^{ER}*Rragb*$^{fl/fl}$ (n = 8) mice. (L) Representative flow plots of GL-7 and Fas expression in lymphocytes from the Peyer's patches from WT (n = 6) and Cre^{ER}*Rragb*$^{fl/fl}$ (n = 7) mice. Data in graphs represent mean ± SEM. ns, not significant. **p < 0.01, ***p < 0.001, and ****p < 0.0001, One-way ANOVA (C and D), two-way ANOVA (J), two-tailed/unpaired Student's t test (E, F, H, I, K, L and G). Source data are provided as a Source Data file.

Supplementary Fig. 2

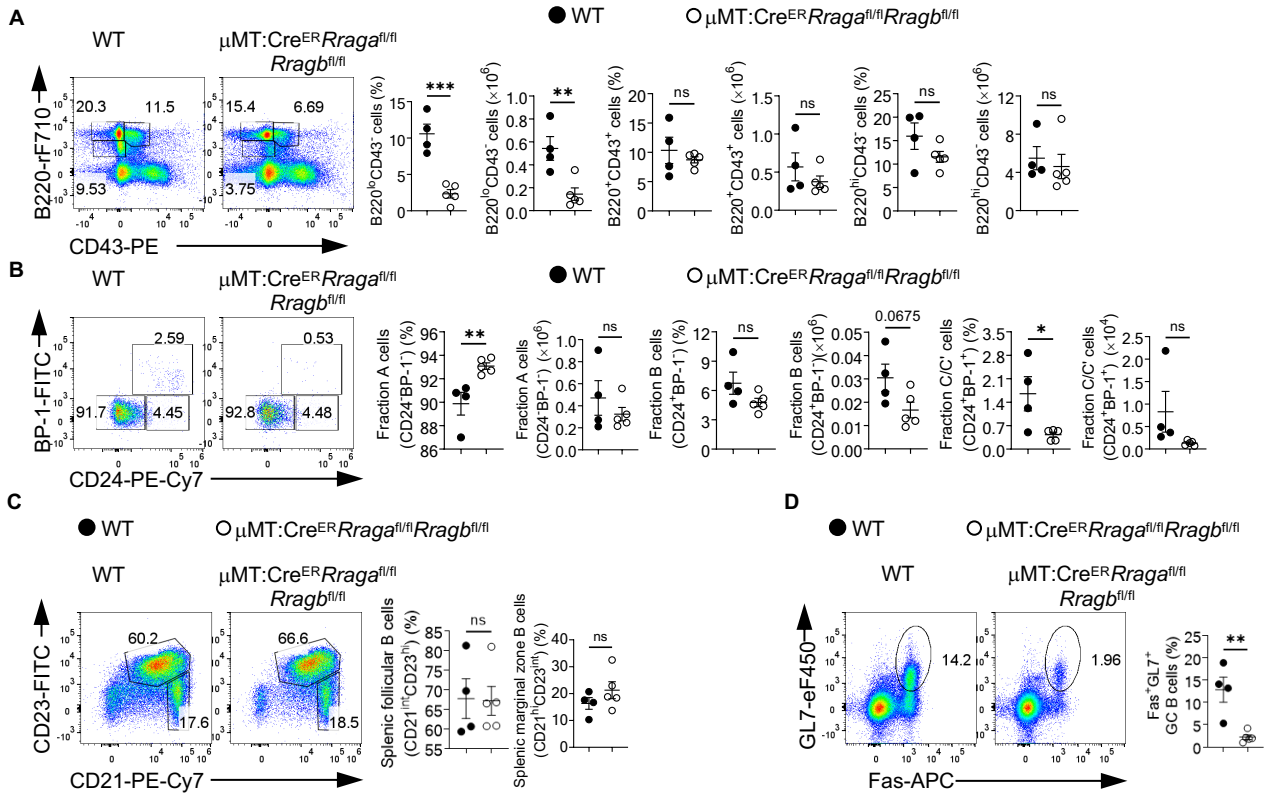

Supplementary Fig. 2. Rag-GTPases deficiency intrinsically disrupts B cell development. (A-D) Tamoxifen was administered to μMT:Cre^{ER}*Rraga*$^{fl/fl}$*Rragb*$^{fl/fl}$ (n = 5), and WT (n = 4) chimera mice by oral gavage daily for 4 consecutive days. Mice were analyzed 7 days after the last injection. (A) Representative flow plots of bone marrow B220 and CD43 expression from μMT:Cre^{ER}*Rraga*$^{fl/fl}$*Rragb*$^{fl/fl}$, and WT chimera mice. Right, summaries of the percentages and numbers of B220^{lo}CD43^{-}, B220^{hi}CD43^{-} and B220^{+}CD43^{+} cells. (B) Representative flow plots of BP-1 and CD24 expression in BM B220^{+}CD43^{+}IgM^{-} B cell precursors from μMT:Cre^{ER}*Rraga*$^{fl/fl}$*Rragb*$^{fl/fl}$, and WT chimera mice. Right, summaries of the percentages and numbers of bone marrow fraction A (CD24^{-}BP-1^{-}), fraction B (CD24^{+}BP-1^{-}), and fraction C/C′(CD24^{+}BP-1^{+}) cells. (C) Representative flow plots of splenic follicular B cells (CD21^{int}CD23^{hi}) or marginal zone (CD21^{hi}CD23^{int}) from μMT:Cre^{ER}*Rraga*$^{fl/fl}$*Rragb*$^{fl/fl}$, and WT chimera mice. Right, summaries of the percentages of splenic follicular B cells (CD21^{int}CD23^{hi}) or marginal zone (CD21^{hi}CD23^{int}) B cells. (D) Representing flow plots of Fas and GL-7 expression on B cells from the Peyer's patches of μMT:Cre^{ER}*Rraga*$^{fl/fl}$*Rragb*$^{fl/fl}$, and WT chimera mice. Right, summary of the percentages of GC (GL-7^{+}Fas^{+}) B cells. Data in graphs represent mean ± SEM. ns, not significant. *p < 0.05, **p < 0.01, ***p < 0.001, two-tailed Student's t test was used.

Supplementary Fig. 3

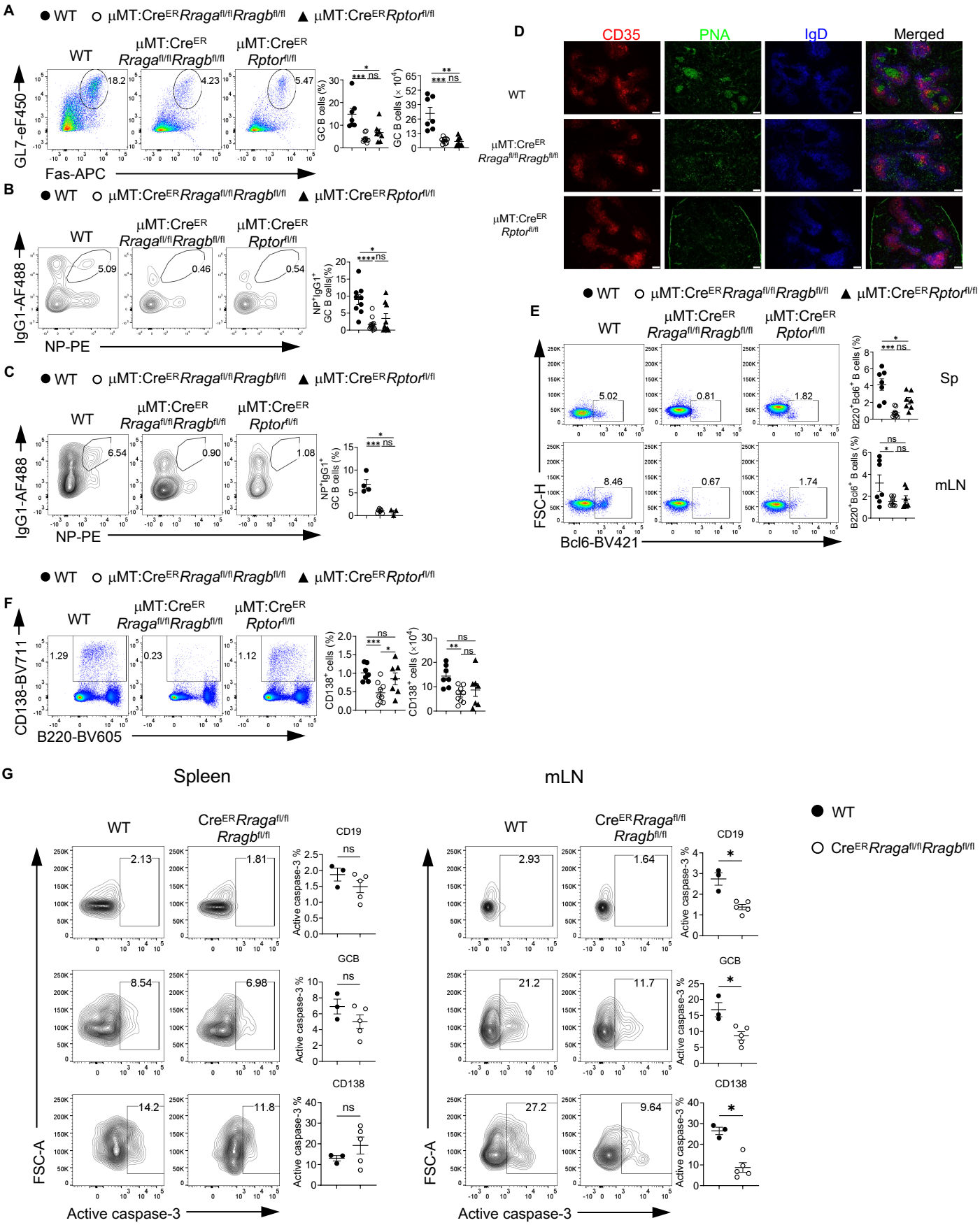

Supplementary Fig. 3. Rag-GTPases deficiency reduces GC formation and antibody production independent of mTORC1 in peptide immunization. (A-G) Tamoxifen was administered to chimera mice by oral gavage daily for 4 consecutive days. Mice were immunized intraperitoneally (100 mg NP-OVA/alum) 7 days after the last injection. (A) Representative flow plots of GL-7 and Fas expression on B cells from the mesenteric lymph node (mLN) of immunized WT (n = 7), μMT:Cre^{ER}*Rraga*$^{fl/fl}$*Rragb*$^{fl/fl}$ (n = 9), and μMT:Cre^{ER}*Rptor*$^{fl/fl}$ (n = 7) chimera mice. (B) Representative flow plots of NP^{+}IgG1^{+} GC B cells from the spleen of immunized WT (n = 9), μMT:Cre^{ER}*Rraga*$^{fl/fl}$*Rragb*$^{fl/fl}$ (n = 13), and μMT:Cre^{ER}*Rptor*$^{fl/fl}$ (n = 9) chimera mice. (C) Representative flow plots of NP^{+}IgG1^{+} GC B cells from the mLN of immunized WT (n = 4), μMT:Cre^{ER}*Rraga*$^{fl/fl}$*Rragb*$^{fl/fl}$ (n = 7), and μMT:Cre^{ER}*Rptor*$^{fl/fl}$ (n = 3) chimera mice. (D) Cryosections from the spleens of immunized WT, μMT:Cre^{ER}*Rraga*$^{fl/fl}$*Rragb*$^{fl/fl}$, and μMT:Cre^{ER}*Rptor*$^{fl/fl}$ chimera mice were stained for GC B cells (anti-PNA). Scale bar, 50 mm. Anti-IgD stains for FoBs, anti-CD35 stains for follicular dendritic cells (LZ). (E) Representative flow plots of Bcl6 expression on total B cells from both spleen (upper panel) and mLN (lower panel) of immunized WT (n = 7), μMT:Cre^{ER}*Rraga*$^{fl/fl}$*Rragb*$^{fl/fl}$ (n = 9), and μMT:Cre^{ER}*Rptor*$^{fl/fl}$ (n = 7) chimera mice. (F) Representative flow plots of CD138 and B220 expression in mLN of WT (n = 7), μMT:Cre^{ER}*Rraga*$^{fl/fl}$*Rragb*$^{fl/fl}$ (n = 9), and μMT:Cre^{ER}*Rptor*$^{fl/fl}$ (n = 7) mice. (G) Active caspase-3 was measured on CD19^{+}, GC and CD138^{+} B cells of spleens and mesenteric lymph nodes (mLN) from immunized chimera mice, WT (n = 3) and μMT:Cre^{ER}*Rraga*$^{fl/fl}$*Rragb*$^{fl/fl}$ (n = 5). Data in graphs represent mean ± SEM. ns, not significant. *p < 0.05, **p < 0.01, ***p < 0.001, and ****p < 0.0001, one-way ANOVA (A-F), two-tailed/unpaired student T-test (G). Source data are provided as a Source Data file.

Supplementary Fig. 4

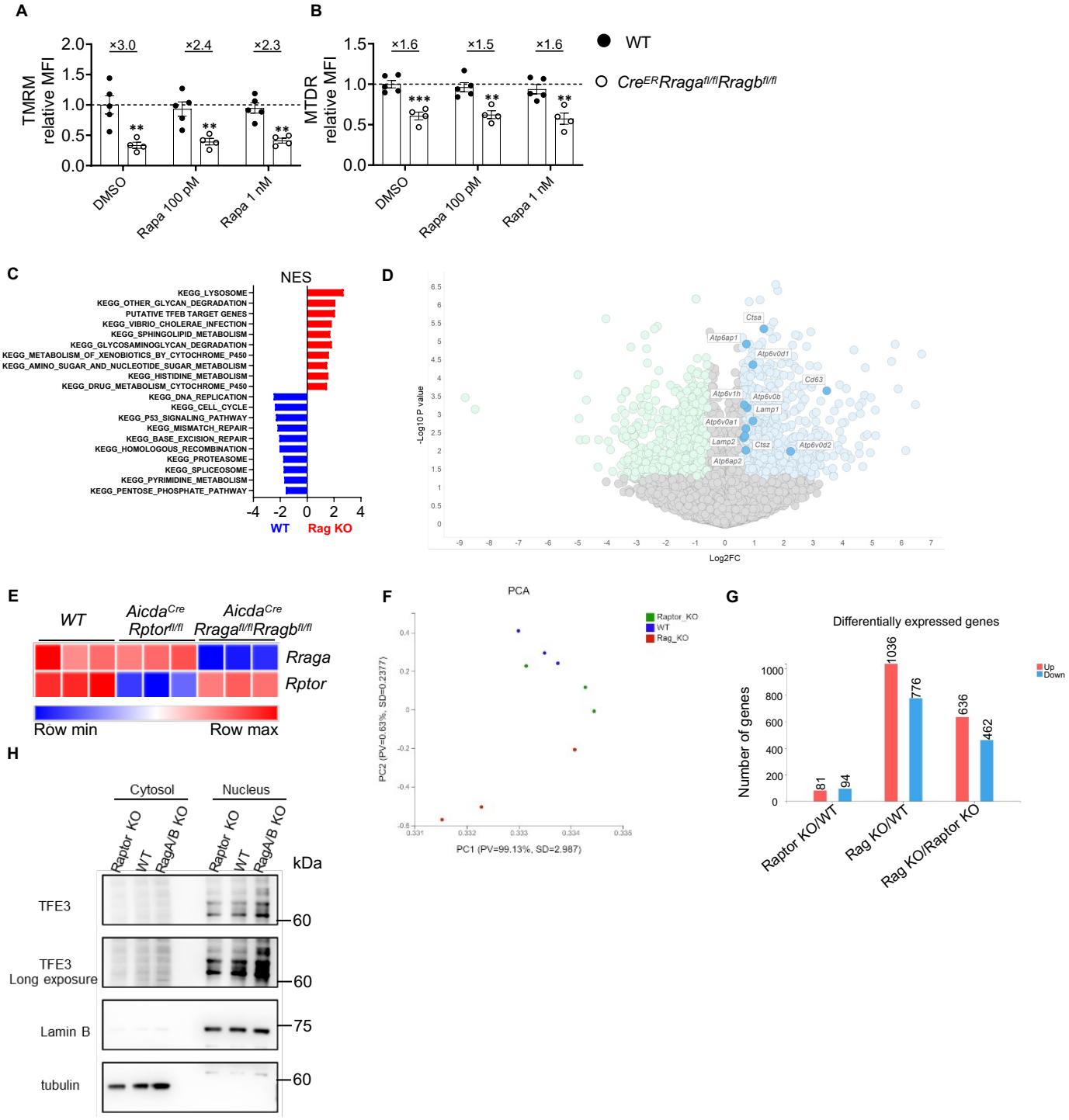

Supplementary Fig. 4. Rag-GTPases regulate TFEB/TFE3 axis in B cells. (A-B) Rapamycin was added into the culture medium at 24 h after B cells were stimulated with LPS/IL-4/BAFF. TMRM (A) or MTDR (B) staining was examined by flow cytometry after B cells were stimulated for additional 48 h, WT (n = 5) and Cre^{ER}*Rraga*$^{fl/fl}$*Rragb*$^{fl/fl}$ (n = 4). The mean fluorescence intensity (MFI) of TMRM and MTDR was normalized to that of WT B cells treated with DMSO (set as "1"). The numbers indicate the fold differences of average TMRM or MTDR MFI between WT and RagA/RagB deficient B cells. Data in graphs represent mean ± SEM. **p < 0.01, ***p < 0.001, two-tailed/unpaired Student's t test (A and B). (C) Bulk RNA sequencing was performed on the B cells activated with LPS/IL-4/BAFF for 72 h, then GSEA was conducted on differentially expressed genes (DEGs), and significantly enriched pathways were plotted according to NES (normalized enrichment score). (D) Volcano plot of the lysosome genes enriched in RagA/RagB deficient B cells. (E-G) GC B cells were sorted from immunized *Aicda*^{Cre}*Rraga*$^{fl/fl}$*Rragb*$^{fl/fl}$, *Aicda*^{Cre}*Rptor*$^{fl/fl}$, and WT mice, and conducted bulk RNA sequencing. (E) *Rraga,* and *Rptor* levels from the bulk RNA sequencing data. (F) PCA plot from the bulk RNA sequencing analysis. (G) Statistics of differently expressed genes from different comparisons. (H) Cytosolic and nuclear proteins were isolated from the B cells activated with LPS/IL-4/BAFF for 72 h. Expression of TFE3 was examined by immunoblot. Lamin B was used as a nuclear control, tubulin was used as a cytosol control. Source data are provided as a Source Data file.

Supplementary Fig. 5

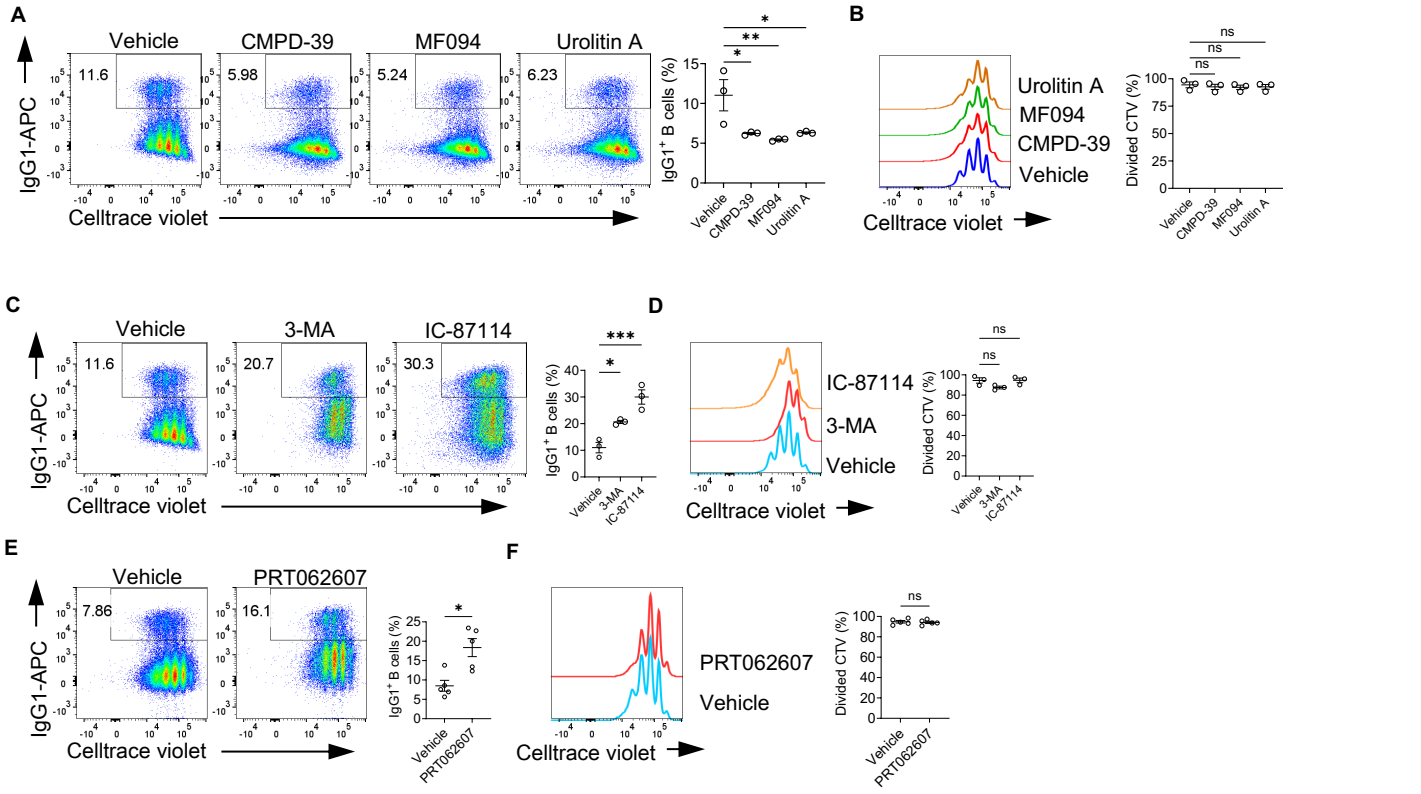

Supplementary Fig. 5. Mitophagy modulates B cell activation. (A and B) B cells were labeled with Celltrace violet (CTV) and stimulated with LPS/IL-4/BAFF in the presence of mitophagy activators CMPA-39 (1 μM), MF094 (1 μM) or Urolitin A (1 μM) for 72 h, IgG1 expression (A) and dilution of CTV (B) were examined by flow cytometry. Right, the percentage of IgG1$^+$ B cells (A) or divided CTV (B). (C-F) B cells were labeled with CTV and stimulated with LPS/IL-4/BAFF and mitophagy inhibitors 3-MA (1 mM), IC-87114 (5 μM) (C and D) or PRT062607 (1 μM) (E and F) for 3 days, IgG1 expression and CTV dilution were measured by flow cytometry. Data presented in the graphs were collected from 3 independent experiments. Data in graphs represent mean ± SEM. ns, not significant. *p < 0.05, **p < 0.01, ***p < 0.001, and, one-way ANOVA (A-D), two-tailed/unpaired student T-test (E and F). Source data are provided as a Source Data file.

Supplementary Fig. 6

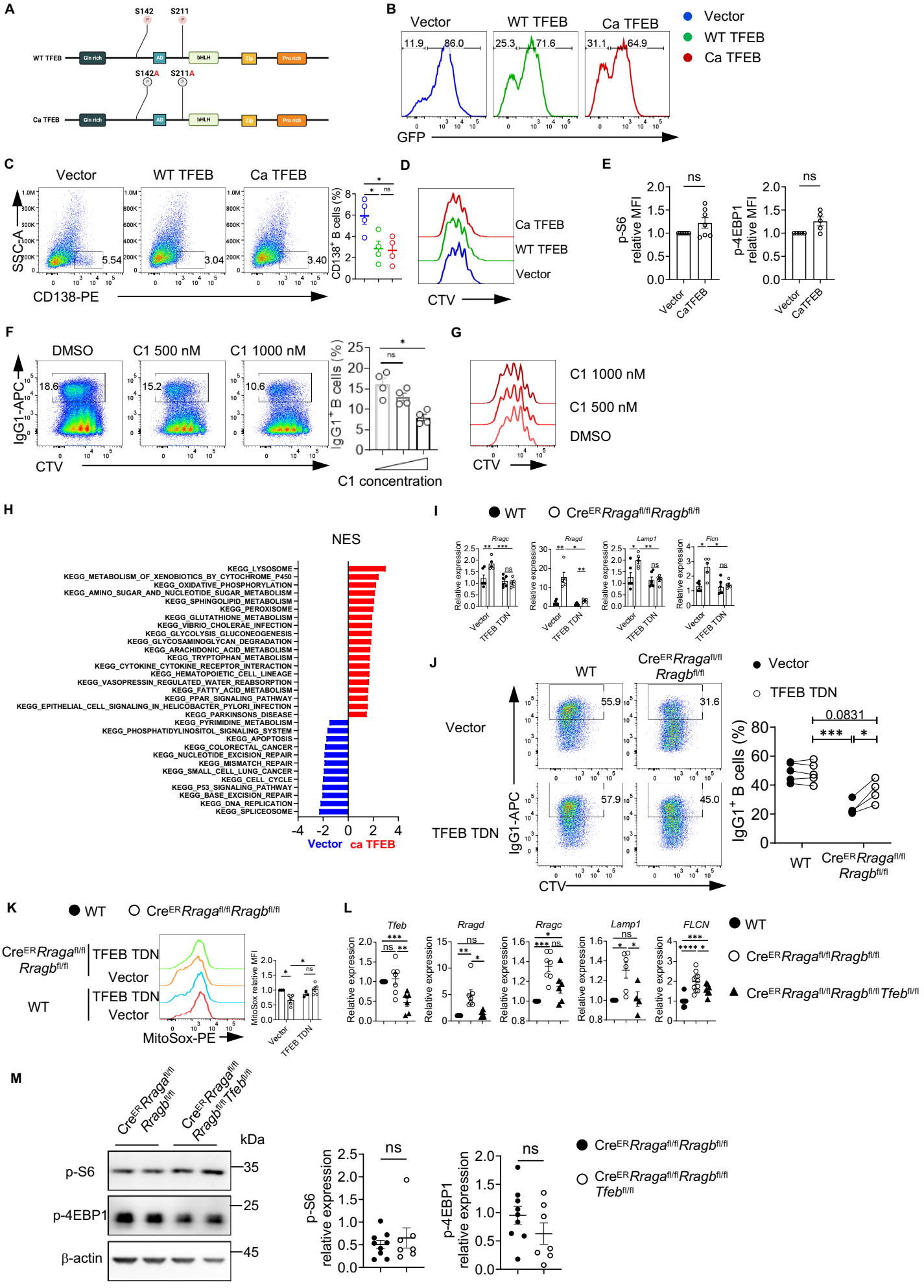

Supplementary Fig. 6. TFEB plays a critical role in Rag GTPases regulated B cell function. (A) Schematic of the experimental design for making WT TFEB and Ca TFEB plasmids (Created in BioRender. Zhu, X. (2023) https://BioRender.com/w00l228). (B) Representative histogram of GFP expression on the vector, WT TFEB or Ca TFEB transduced B cells. (C) Representative flow plots of $CD138^+$ expression on vector, WT TFEB, and Ca TFEB transduced GFP^+ B cells, n = 4 for each group. (D) Representative flow plots of CTV dilution from vector, WT TFEB, and Ca TFEB transduced GFP^+ B cells. (E) p-S6 (n = 7 per group) and p-4EBP1(n = 5 per group) levels were measured on GFP^+ B cells by flow cytometry and the relative MFI was presented. (F) Representative flow plots of IgG1 and CTV expression activated in LPS/IL-4/BAFF with different concentrations of compound C1 for 72 h, n = 4 for each condition. (G) Representative flow plots of CTV dilution from different concentrations of compound C1 treated B cells. (H) Significantly enriched pathways were plotted according to NES. (I) Splenic B cells from Cre^{ER}*Rraga*$^{fl/fl}$*Rragb*$^{fl/fl}$ (n = 5), and WT (n = 5) mice were transduced with vector or TFEB TDN, and TFEB downstream target genes were examined on GFP^+ B cells. (J) Splenic B cells from were transduced with vector or TFEB TDN, $IgG1^+$ B cells and MitoSox were measured. For $IgG1^+$ B cells, Cre^{ER}*Rraga*$^{fl/fl}$*Rragb*$^{fl/fl}$ (n = 4), and WT (n = 5) mice. For MitoSox, Cre^{ER}*Rraga*$^{fl/fl}$*Rragb*$^{fl/fl}$ (n = 5), and WT (n = 3) . (K) TFEB downstream target genes were measured on the activated B cells. For *Tfeb*, *Rragc* and *Rragd*, WT (n = 6), Cre^{ER}*Rraga*$^{fl/fl}$*Rragb*$^{fl/fl}$ (n = 7), and Cre^{ER}*Rraga*$^{fl/fl}$*Rragb*$^{fl/fl}$*Tfeb*$^{fl/fl}$ (n = 6) mice. For *Lamp1*, WT (n = 4), Cre^{ER}*Rraga*$^{fl/fl}$*Rragb*$^{fl/fl}$ (n = 5), and Cre^{ER}*Rraga*$^{fl/fl}$*Rragb*$^{fl/fl}$*Tfeb*$^{fl/fl}$ (n = 4). For *Flcn*, WT (n = 11), Cre^{ER}*Rraga*$^{fl/fl}$*Rragb*$^{fl/fl}$ (n = 11), and Cre^{ER}*Rraga*$^{fl/fl}$*Rragb*$^{fl/fl}$*Tfeb*$^{fl/fl}$ (n = 7). (M) p-S6 and p-4EBP1 levels were measured on activated B cells by immunoblot, Cre^{ER}*Rraga*$^{fl/fl}$*Rragb*$^{fl/fl}$ (n = 9), and Cre^{ER}*Rraga*$^{fl/fl}$*Rragb*$^{fl/fl}$*Tfeb*$^{fl/fl}$ (n = 7). Data in graphs represent mean ± SEM. ns, not significant. *p < 0.05, **p < 0.01, and ***p < 0.001, one-way ANOVA (C, F and L), two-way ANOVA (I-K), two-tailed/unpaired student T-test (E and M). Source data are provided as a Source Data file.

Supplementary Fig. 7

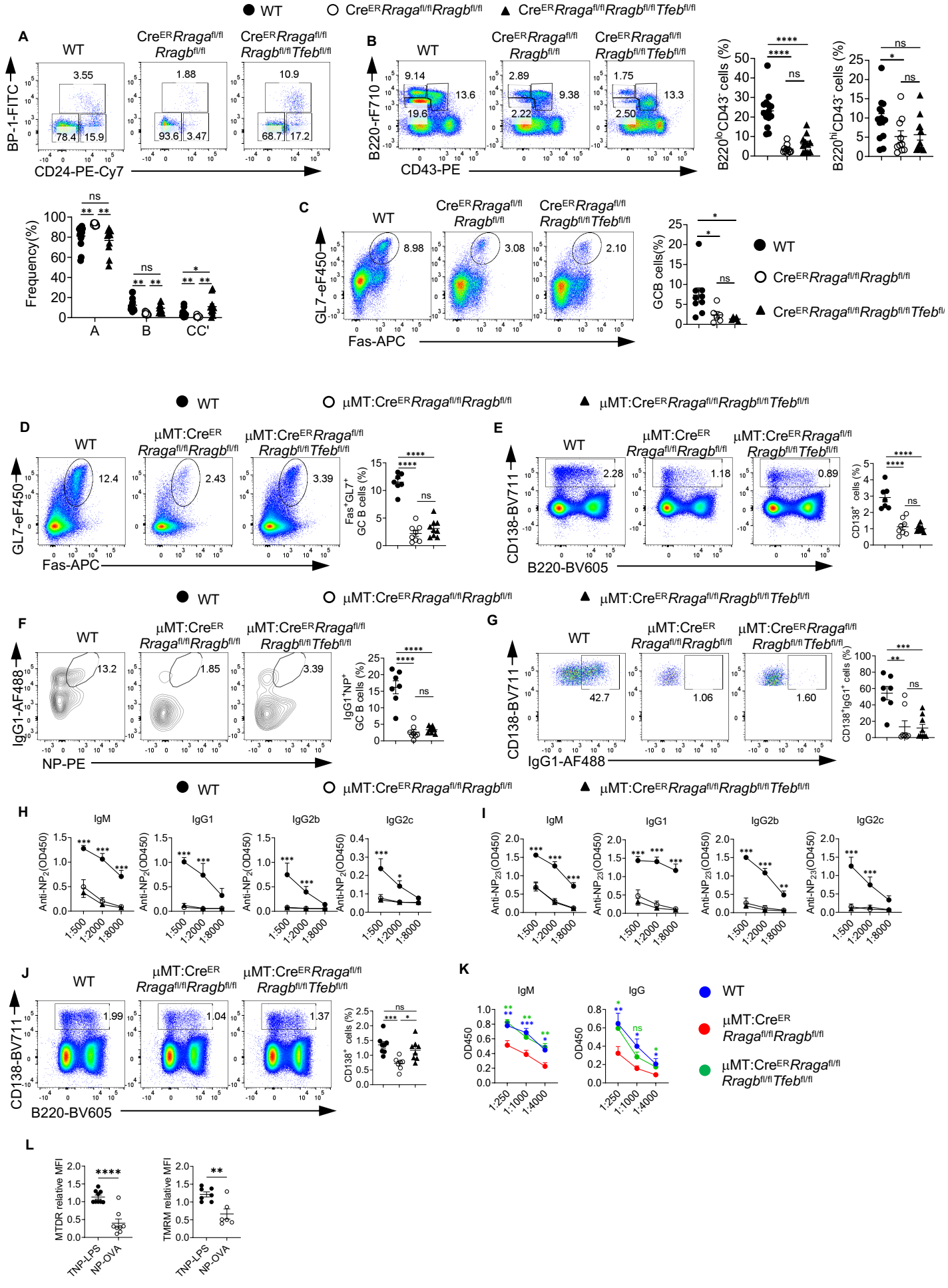

Supplementary Fig. 7. Abrogating TFEB rescues the deficiency in Rag-GTPases KO mice in context-dependent manner. (A) Representative flow plots of BP-1 and CD24 expression in BM $B220^{+}CD43^{+}IgM^{-}$ B cell precursors from WT (n = 14), $Cre^{ER}Rraga^{fl/fl}Rragb^{fl/fl}$ (n = 10), and $Cre^{ER}Rraga^{fl/fl}Rragb^{fl/fl}Tfeb^{fl/fl}$ (n = 11) mice. (B) Representative flow plots of B220 and CD43 expression in BM lymphocytes from $Cre^{ER}Rraga^{fl/fl}Rragb^{fl/fl}$ (n = 10), $Cre^{ER}Rraga^{fl/fl}Rragb^{fl/fl}Tfeb^{fl/fl}$ (n = 11), and WT (n = 14) mice. (C) Representative flow plots of GL-7 and Fas expression in lymphocytes from the Peyer's patches of WT (n = 9), $Cre^{ER}Rraga^{fl/fl}Rragb^{fl/fl}$ (n = 6), and $Cre^{ER}Rraga^{fl/fl}Rragb^{fl/fl}Tfeb^{fl/fl}$ (n = 5) mice. (D-I) Tamoxifen was administered to animals by oral gavage daily for 4 consecutive days. Mice were immunized intraperitoneally (100 mg NP-OVA/alum) 7 days after the last injection. (D) Representative flow plots of GL-7 and Fas expression on splenic B cells from the spleen of WT (n = 7), $\mu MT{:}Cre^{ER}Rraga^{fl/fl}Rragb^{fl/fl}$ (n = 8), and $\mu MT{:}Cre^{ER}Rraga^{fl/fl}Rragb^{fl/fl}Tfeb^{fl/fl}$ (n = 9) immunized chimera mice. (E) Representative flow plots of CD138 and B220 expression in spleens from immunized WT (n = 7), $\mu MT{:}Cre^{ER}Rraga^{fl/fl}Rragb^{fl/fl}$ (n = 8), and $\mu MT{:}Cre^{ER}Rraga^{fl/fl}Rragb^{fl/fl}Tfeb^{fl/fl}$ (n = 9) chimera mice. (F) Representative flow plots of $NP^{+}IgG1^{+}$ GC B cells from the spleen of immunized WT (n = 7), $\mu MT{:}Cre^{ER}Rraga^{fl/fl}Rragb^{fl/fl}$ (n = 9), and $\mu MT{:}Cre^{ER}Rraga^{fl/fl}Rragb^{fl/fl}Tfeb^{fl/fl}$ (n = 9) chimera mice. (G) Representative flow plots of splenic $CD138^{+}IgG1^{+}$ cells from immunized WT (n = 7), $\mu MT{:}Cre^{ER}Rraga^{fl/fl}Rragb^{fl/fl}$ (n = 8), and $\mu MT{:}Cre^{ER}Rraga^{fl/fl}Rragb^{fl/fl}Tfeb^{fl/fl}$ (n = 9) chimera mice. (H) high-affinity NP-specific antibodies of all classes were measured using the sera of immunized WT (n = 6), $\mu MT{:}Cre^{ER}Rraga^{fl/fl}Rragb^{fl/fl}$ (n = 8), and $\mu MT{:}Cre^{ER}Rraga^{fl/fl}Rragb^{fl/fl}Tfeb^{fl/fl}$ (n = 9) chimera mice. (I) Total NP-specific antibodies of all classes were measured using the sera of immunized WT (n = 6), $\mu MT{:}Cre^{ER}Rraga^{fl/fl}Rragb^{fl/fl}$ (n = 8), and $\mu MT{:}Cre^{ER}Rraga^{fl/fl}Rragb^{fl/fl}Tfeb^{fl/fl}$ (n = 9) chimera mice. (J) Representative flow plots of splenic $CD138^{+}$ cells from TNP-LPS immunized WT (n = 8), $\mu MT{:}Cre^{ER}Rraga^{fl/fl}Rragb^{fl/fl}$ (n = 7), and $\mu MT{:}Cre^{ER}Rraga^{fl/fl}Rragb^{fl/fl}Tfeb^{fl/fl}$ (n = 8) chimera mice. (K) anti-TNP antibody titers in the sera of immunized WT (n = 8), $\mu MT{:}Cre^{ER}Rraga^{fl/fl}Rragb^{fl/fl}$ (n = 7), and $\mu MT{:}Cre^{ER}Rraga^{fl/fl}Rragb^{fl/fl}Tfeb^{fl/fl}$ (n = 8) chimera mice. (L) WT mice were immunized with TNP-LPS or NP-OVA/alum, TMRM or MTDR on $CD138^{+}$ cells were measured at day 9 (NP-OVA/alum) or 7 (TNP-LPS) post-immunization. Data in graphs represent mean ± SEM. ns, not significant. *p < 0.05, **p < 0.01, ***p < 0.001, and ****p < 0.0001, one-way ANOVA (B, C, D, E, F, G and J), two-way ANOVA (A, H, I and K), two-tailed/unpaired Student's t test (L). Source data are provided as a Source Data file.

Supplementary Fig. 8

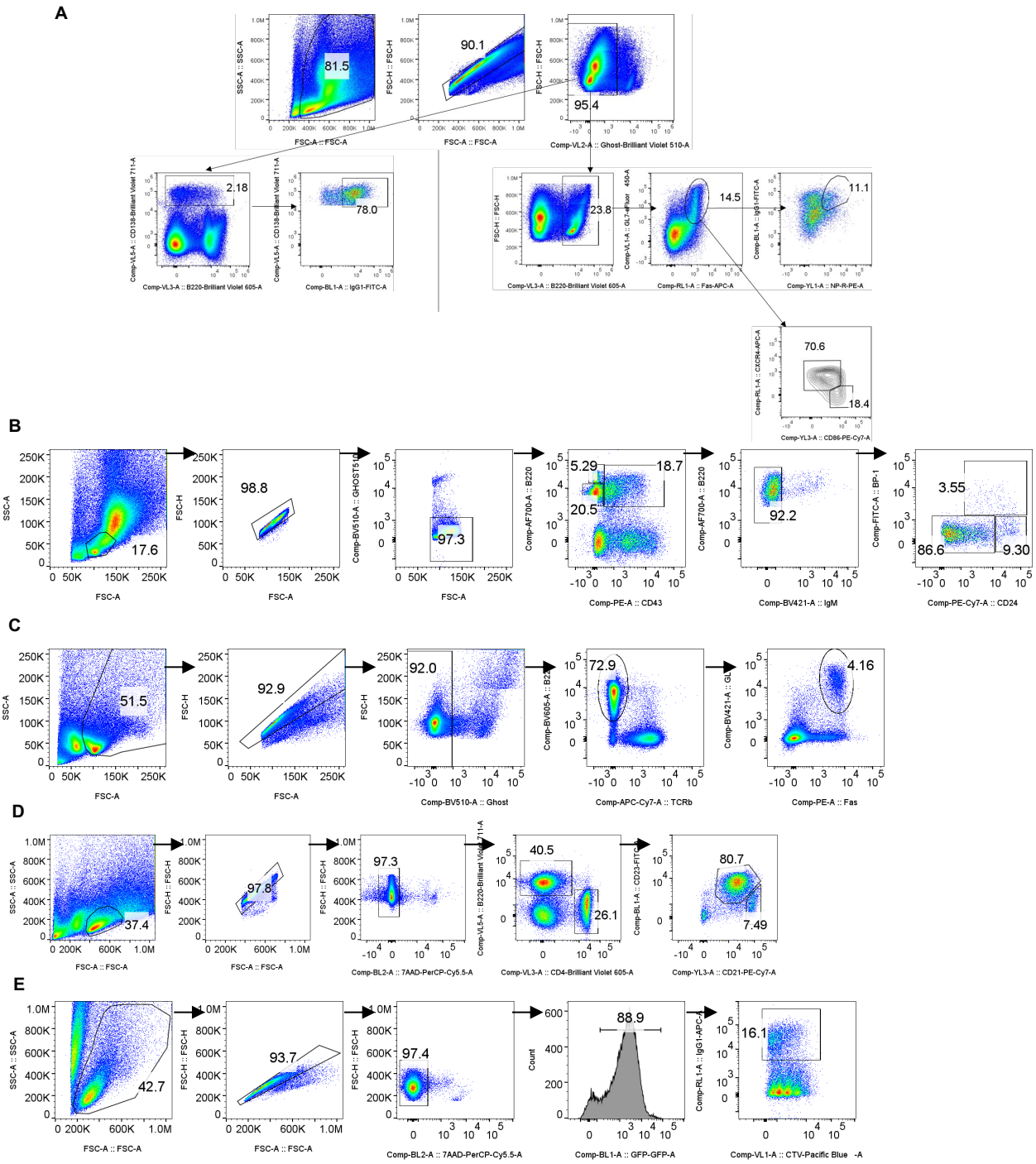

Supplementary Fig. 8 Gating strategies for FACS. (A) B cell analysis from the spleen or mLN of immunized mice, which is related to Fig. 3A-3C, Fig. 3H-3L, Fig. 7I-7K, Supplementary Fig. 3A-3C and 3E-3G, Supplementary Fig. 7D-7G, and 7J. (B) Hardy fraction gating strategy of Bone marrow, which is related to Fig. 2A-2D, Fig. 2H-2L, Fig. 7A-7B; Supplementary Fig. 1I-7J; Supplementary Fig. 2A-2B; Supplementary Fig. 7A-7B. (C) Germinal center B cell analysis in the Peyer's patch, which is related to Fig. 2E, Fig. 7C, Supplementary Fig. 1L, Supplementary Fig. 2D, Supplementary Fig. 7C. (D) Follicular and marginal zone B cells were analyzed in the spleen, which is related to Supplementary Fig. 1C-1D and 1K, Supplementary Fig. 2C. (E) Virally transduced B cells were analyzed/sorted by flow cytometery, which is related to Fig. 6B-6K, Supplementary Fig. 6B-6K.

Supplementary table

Gene	Name	Primer sequence
β-actin	β-actin-F	CGTCGACAACGGCTCCGGCATG
	β-actin-R	GGGCCTCGTCACCCACATAGGAG
Flcn	Flcn-F	GATGACAACTTGTGGGCGTGTC
	Flcn-R	CATCTGGACCAGGGTGTCCTCT
Tfeb	Tfeb-F	CCACCCCAGCCATCAACAC
	Tfeb-R	CAGACAGATACTCCCGAACCTT
Rragd	Rragd-F	CTGTTTGACGTGGTCAGTAAGAT
	Rragd-R	GTTGAGTCCTTGTCATACGGG
Lamp1	Lamp1-F	CAGCACTCTTTGAGGTGAAAAAC
	Lamp1-R	ACGATCTGAGAACCATTCGCA
Rragc	Rragc-F	AGATGTCACCCAATGAGACTCT
	Rragc-R	AGTCGTCCTGTGCATCAATGA